Generation of Trains of Electron Microbunches with Adjustable Subpicosecond Spacing

P. Muggli,[1] V. Yakimenko,[2] M. Babzien,[2] E. Kallos,[1] and K. P. Kusche[2]
[1]University of Southern California, Los Angeles, California 90089, USA
[2]Brookhaven National Laboratory, Upton, Long Island, New York 11973, USA
(Received 25 December 2007; published 29 July 2008)

We demonstrate that trains of subpicosecond electron microbunches, with subpicosecond spacing, can be produced by placing a mask in a region of the beam line where the beam transverse size is dominated by the correlated energy spread. We show that the number, length, and spacing of the microbunches can be controlled through the parameters of the beam and the mask. Such microbunch trains can be further compressed and accelerated and have applications to free electron lasers and plasma wakefield accelerators.

DOI: 10.1103/PhysRevLett.101.054801 PACS numbers: 41.75.Ht, 41.75.Lx, 52.40.Mj

Short, high-brightness electron bunches play a key role in producing ultrashort pulses of coherent x-ray radiation in free electron lasers (FELs) [1] and in exciting ultrahigh accelerating gradients in plasma wakefield accelerators (PWFAs) [2]. Single short electron bunches most often are obtained by magnetic compression [3] or by velocity bunching [4,5]. However, the performances and characteristics of FELs and PWFAs could be greatly extended by driving them with a train of short microbunches rather than with a single bunch.

In the FEL case, microbunches with energy increasing or decreasing along the train could produce a corresponding train of radiation pulses of variable delays and wavelengths, with potential applications to ultrafast pump-probe experiments at the femtosecond time scale [6].

In a PWFA driven by a single electron bunch, the peak accelerating field is, in principle, limited to twice the value of the peak decelerating field within the bunch [7]. Therefore, the maximum possible energy gain for trailing particles, or for a witness bunch, is less than twice the incoming energy. However, recent proof-of-principle, single-bunch experiments in the nonlinear regime of the PWFA have shown that, in practice, the energy of trailing particles is *only doubled* (i.e., the energy gain equal to the input energy) [2]. Several methods were proposed to increase the accelerating field [8,9]. One, which is applicable to all collinear wakefield accelerators, is known as the ramped bunch train method [10] and consists of using a train of equidistant bunches wherein the charge increases along the train. This method was recently used in a dielectric-loaded accelerator (DLA) in the microwave range to show for the first time that the accelerating wakefield can be increased by a factor of 1.31 when driven by two bunches separated by the proper distance and with the proper relative charges [11]. However, in these DLA experiments the bunches were separated by many radio-frequency wavelengths, i.e., by many centimeters. These bunches were produced by splitting and then delaying the laser pulse that generates the electrons in the photocathode gun. For PWFAs, however, the plasma wavelength λ_p typically is of the order of a few tens or hundreds of microns, and the wakefield tends to lose its coherence after a few periods [12]. Consequently, producing bunch trains suitable for these advanced accelerators is very challenging.

For these new applications, it is essential to create trains of high-brightness femtosecond microbunches with stable length, charge, and spacing; the spacing between them need not be equidistant. Wake excitation by trains of microbunches has recently been considered numerically in the context of a multibunch electron-positron collider [13].

The method presented here employs a masking technique to produce a train of microbunches with controllable spacing and width; advantageously, it can be adapted to future FEL or PWFA experiments using high-energy beams. It can be applied to beams at their intermediate energy level (0.5–1 GeV, larger than the 58 MeV of the experiments described here) where the beam can be focused to small transverse sizes ($\sigma_{x,y} \approx 1/\gamma^{1/2}$, γ the beam relativistic factor). After generating the microbunch train, it can, in principle, be further compressed in a subsequent magnetic chicane and then accelerated. Although a significant fraction of the beam charge is lost after the mask, this loss occurs at relatively low energy when compared to its final multi-GeV energy and therefore does not significantly reduce the beam generation efficiency. This particle loss also induces only modest activation of the beam line. Bunches with multi-nC charge have been produced by photoinjector guns, although with relatively large emittance [14,15]. The total charge in the train after the mask could therefore also be in the multi-nC range, even when considering a mask transmission $<50\%$. Methods were proposed to produce such trains of microbunches [16–18]. However, we present here the first successful experimental realization of such a method. A time structure can be ''cut out'' from a bunch by changing the electrons' energy to an extent large enough that they could be separated from the main beam or even completely stopped by the mask itself [16]. In contrast, in the method presented here the particles are selected based on the scattering of their emittance at the mask.

In this Letter, we describe the first experimental demonstration of the generation of a stable train of microbunches with a controllable subpicosecond delay. We produce the microbunch train by imprinting the shadow of a periodic mask onto a bunch with a correlated energy spread (see cartoon in Fig. 1). The mask is placed in a region of the beam line where the beam transverse size is dominated by this correlated energy spread. The mask spoils the emittance of particles that strike its solid parts, and these particles are subsequently lost along the beam transport line. The shadow of the mask then is converted into a time pattern when entering the dispersion-free region of the beam line. We measure this time pattern using coherent transition radiation (CTR) interferometry. We demonstrate the ability to produce trains with different numbers of microbunches and different spacings. Such a simple method can be implemented in any accelerator that includes a magnetic chicane or dogleg. It can be used in conjunction with magnetic compression to produce trains of ultrashort electron microbunches.

At the Brookhaven National Laboratory (BNL) Accelerator Test Facility (ATF), the electron beam is produced in a 1.6-cell, S-band, high-brightness rf-photoinjector gun [19], which is followed by an S-band linear accelerator or linac. The electron bunch has a typical normalized emittance ϵ_N of $\approx$2 mm mrad and a charge of $\approx$500 pC. In the linac, the beam is also accelerated off the crest of the radio-frequency wave in order to impart a correlated energy spread on the bunch [typically $\Delta E/E_0 \approx \pm(0.5\text{–}1)\%$]. The beam mean energy is $E_0 = 58$ MeV. Two dipole and five quadrupole magnets are arranged in a dogleg configuration, as seen in Fig. 2. Before the dogleg, the bunch is $\sigma_z \approx 1650$ μm long (or ≈ 5.5 ps, full width of the core). The dogleg longitudinal dispersion function R_{56} is ≈ -4 cm [20]; hence, it can either compress or stretch the bunch by ± 400 μm per percent of correlated energy spread (or ± 1.3 ps), depending on the sign of the energy chirp.

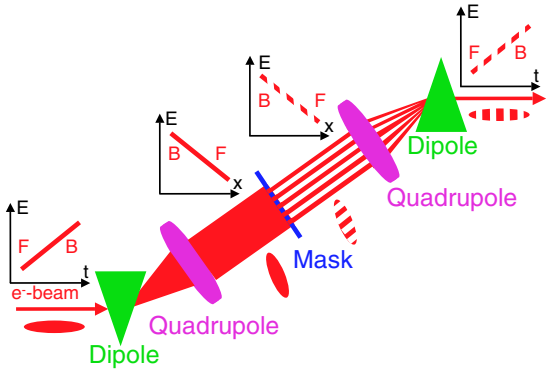

FIG. 1 (color online). Simplified schematic of the mask principle. Only the dogleg section of the beam line is depicted (not to scale), and three quadrupole magnets are omitted. The side graphs represent the beam energy correlation with the beam front labeled by "F" and the back by "B."

The beam beta functions β_x and β_y ($\beta_{x,y} = \gamma\sigma_{x,y}^2/\epsilon_N$, $\sigma_{x,y}$ are the transverse beam sizes in the x and y planes) as well as the magnetic dispersion η_x ($\eta_y = 0$) as obtained with the beam propagation code MAD [21] are shown in Fig. 2. The beam sizes and the dispersion were measured at various locations along the beam line and were within $\approx \pm 10\%$ of the predicted values of Fig. 2. The dogleg quadrupole magnets are adjusted to obtain two regions of large dispersion and low beta function. This condition ensures that at these locations the beam size due to its correlated energy spread is much larger than that due to its emittance, i.e., $\sigma_\eta = \eta_x|\Delta E/E_0| \gg \sigma_x = (\beta_x\epsilon_N/\gamma)^{1/2}$. Hence, its energy can be selected. Furthermore, at these locations the time-correlated energy spread also corresponds to a transverse position or energy correlation, and therefore modulating the beam in its energy plane is equivalent to modulating the beam in time. A limiting slit aperture is placed at the first small σ_x location ($s = 10.8$ m, Fig. 2, s is the distance along the beam line), where the dispersion is $\eta_{x,\text{slit}} \approx -0.60$ m and $\sigma_x \approx 85$ μm. This slit, with a variable width, restricts the energy spectrum of the bunch and thereby the number of microbunches in the train, as explained below.

The mask is placed at the second small σ_x location ($s = 16.6$ m, Fig. 2), where $\eta_{x,\text{mask}} \approx +1.4$ m. For these proof-of-principle experiments, the mask consists of a series of equidistant circular steel wires of diameter $d = 500$ μm, or about 1/35 of a radiation length, separated by a period $D = 1270$ μm. The wires are stretched along the y axis. The emittance associated to the fraction of the beam scattered by the solid parts of the mask increases by a factor of more than 100, but electrons lose only a small fraction of their energy (less than $\approx 3\%$). Once the beam leaves the dogleg, the dispersion is brought back to zero, and the

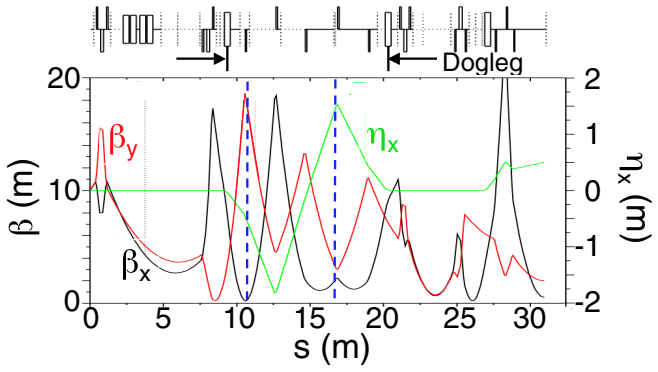

FIG. 2 (color online). Beam beta functions (β_x black, β_y red line), and dispersion in the x plane η_x (green line), obtained using the MAD program. The dashed blue lines represent the location of the energy slit (left-hand side) and of the mask (right-hand side). The beam line elements are shown in the figure above the graph. Quadrupoles focusing in the y (x), vertical (horizontal) plane are indicated by thin rectangles above (below) the middle line, dipoles by full rectangles across the line, and beam profile monitors by the dotted lines.

mask pattern is converted into a pure time pattern of microbunches. The beam then propagates over a dispersion-free distance of ≈ 6.5 m, wherein experiments can be performed, before entering a magnetic spectrometer with a final dispersion of $\eta_x \approx 0.5$ m where the beam energy spectrum is measured. The large emittance time slices of the bunch are lost along the beam line before reaching the experimental location. Note that a fraction $\approx d/D$ of the beam charge is lost after it passes the mask. Note also that, in order for the mask to cast a crisp shadow, the transverse size of the beam at the mask due to its emittance only must also be smaller than the wire size: $\sigma_x = (\beta_x \epsilon_N/\gamma)^{1/2} \ll d$. At the mask $\beta_x = 1.9$ m (see Fig. 2), $\sigma_x = 182$ μm; therefore, the condition $\sigma_x \ll d$ is marginally satisfied in this case. However, not meeting this requirement does not affect the microbunches spacing or its measurement.

Figure 3 shows energy spectra for the case of a correlated energy spread of $\Delta E/E_0 \approx 0.5\%$. The spectra show the shadow of the mask with six and seven microbunches, as determined by two different limiting slit widths, and demonstrate the ability to generate trains with different numbers of microbunches. Here the incoming bunch's temporal charge profile determines the charge in each individual microbunch. The microbunches' charge can be controlled by another limiting slit with a variable width or a mask placed perpendicularly to the mask wires.

The broadband transition radiation emitted by the electrons when entering a copper mirror placed after the dogleg, near the experimental region, is sent to a Martin-Puplett interferometer. The transition radiation at wavelengths shorter than the microbunch length σ_{zm} ($\lambda \ll 2\pi\sigma_{zm}$) is emitted incoherently, while the long wavelengths ($\lambda \gg 2\pi\sigma_{zm}$) are emitted coherently and, in principle, carry information about the microbunches' number, spacing, and length [22]. Such long wavelengths interfere in the interferometer. The total energy of the interference signal is recorded by a liquid helium cooled silicon bolometer as a function of the difference in path length between the interferometer arms. Thus, the interferometer signal yields the autocorrelation trace of the microbunch train. A train of N equidistant microbunches is expected to yield a trace with $(2N + 1)$ peaks. Figure 4 displays autocorrelation traces obtained with two incoming bunch parameters with total energy spreads of 1.5% and 3.5%, respectively, and $N = 3$ and $N = 4$ microbunches, respectively, as determined by the limiting slit widths and as observed on bunch energy spectra similar to those of Fig. 3 (not shown). The number of peaks in the autocorrelation traces is 5 and 7, in agreement with the expected $(2N + 1)$ peaks. The microbunches' spacing Δz is directly deduced from the path length difference between the peaks [Fig. 4(b)] and corresponds to 434 ± 22 and 216 ± 60 μm (or ≈ 1.45 and ≈ 720 fs), respectively. The microbunches carry ≈ 18 and ≈ 8 pC, respectively, and a current of $\approx 18A$ in both cases.

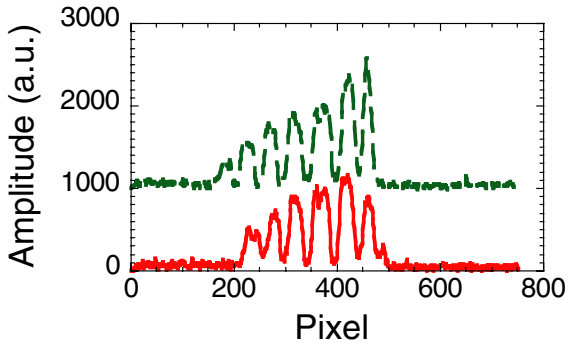

FIG. 3 (color online). Profiles of the beam dispersed in energy at the end of the beam line with the energy slit allowing either 6 (red line) or 7 microbunches (dashed green line, shifted up by 1000 a.u.), which demonstrate the ability to choose the number of microbunches in the train. Variations in the microbunches' amplitudes reflect slightly different beam tuning and incoming temporal bunch charge or current profile.

The distance between the microbunches is given by the bunch length when exiting the dogleg: $\sigma_z' = \sigma_z \pm R_{56}\Delta E/E_0$ divided by the number of microbunches in the full bunch train (with the limiting slit fully open). The number of microbunches is determined by the transverse size of the beam at the mask: $\sigma_\eta = \eta_{x,\mathrm{mask}}|\Delta E/E_0|$ (for $\sigma_\eta \gg \sigma_x$). Therefore, the microbunches' spacing Δz is $\Delta z = D\frac{\sigma_z \pm R_{56}\Delta E/E_0}{\eta_{x,\mathrm{mask}}|\Delta E/E_0|}$. This expression correctly predicts the measured bunch spacing for the case when the dogleg stretches the incoming bunch ($-$ sign of the $\pm$ in the above equation). Note that the autocorrelation traces of Fig. 4 extend below the level for a large path length difference (>1500 μm on Fig. 4): This results from the long wavelength filtering imposed by the CTR collection system and the limited response of the detector for $\lambda > 1$ mm. However, these limitations do not influence the Δz measurement but prevent that of the microbunches' length. For $\sigma_x \ll d$, the microbunches' length is $\sigma_{zm} = T\Delta z$, where $T = (D - d)/D$ is the mask transparency (≈ 0.6 here), and the time pattern is similar to the mask pattern. For these experiments, $\sigma_x/d \approx 0.364$, and calculations indicate that the microbunches have a Gaussian-like rather than a square shape, with approximately the same full width at half maximum. An important parameter for some applications is the equidistance of the microbunches. Calculations of the autocorrelation trace for a train of square microbunches show that the contrast of the autocorrelation trace and the number of visible peaks significantly decrease when a variation of more than 3% (for a train with seven bunches, as in Fig. 3) in the bunch-to-bunch spacing is included. This was also verified experimentally by making the correlated energy spread nonlinear along the bunch and therefore the microbunches nonequidistant. Thus, the approximately linear increase in the amplitude of the peaks apparent in Fig. 4 is a good indication that the microbunches are equidistant. Also note that the autocorrelation traces were constructed from over 100 consecutive CTR energy mea-

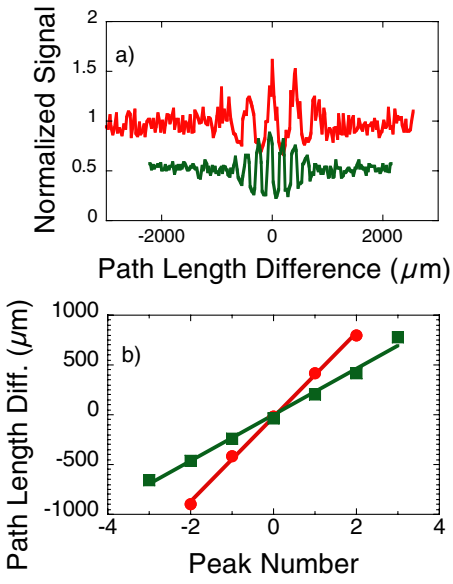

FIG. 4 (color online). (a) Normalized CTR traces obtained with two different incoming full energy spectra: $\Delta E/E_0 \approx 1.5\%$ (red line, shifted up by 0.5 a.u. after normalization) and 3.4% (green line) and with different energy slit width, leading to trains with 3 and 4 microbunches, respectively. The two traces clearly show the dependency of Δz on the incoming correlated energy spread. The distance between the peaks is determined from the slope of a linear fit of the measured path length difference versus peak number shown in (b).

surements, showing that the bunch train structure is indeed stable in time.

The results presented herein with a low-energy, low charge beam demonstrate that a train with an adjustable number of subpicosecond microbunches separated by <1 ps can be produced using a masking technique. For particular applications (such as PWFAs and FELs), the temporal shape and amplitude of the microbunch train can therefore be controlled by the mask pattern and the beam and beam line characteristics at the mask. For these applications, the loss of charge implied by this technique does not significantly reduce the efficiency of producing a high-energy microbunch train. Placing the mask in a 0.5–1 GeV section of the beam line will take advantage of the ability to better focus the beam at higher energies (adiabatic emittance damping), $\sigma_x = (\beta_x \epsilon_N/\gamma)^{1/2}$. Note that the scattering angle also decreases with increasing beam energy. However, the mask thickness can be adjusted to compensate for this effect, and an emittance growth smaller than the one obtained in this experiment is sufficient to selectively eliminate the scattered electrons. Since the mask is a fixed physical object, the stability of the microbunch train is guaranteed by the stability of the dispersion at the mask and that of the beam energy correlation. Both parameters are very stable in a feedback-assisted, high-repetition rate (>10 Hz) accelerator. The microbunch train produced at the BNL-ATF will be used for proof-of-principle multibunch PWFA experiments [23]. The mask will be designed to produce a train of equidistant drive bunches followed by a witness bunch at a distance appropriate to sample the accelerating wakefield and short enough to produce an accelerated beam with a finite energy spread.

This work was supported by the U.S. Department of Energy Grants No. DE-FG02-04ER41294, No. DE-AC02-98CH10886, No. DE-FG03-92ER40695, and No. DE-FG02-92ER40745. We greatly appreciate the contribution of the ATF technical staff to this work.

[1] C. Pellegrini *et al.*, Nucl. Instrum. Methods Phys. Res., Sect. A **331**, 223 (1993).
[2] I. Blumenfeld *et al.*, Nature (London) **445**, 741 (2007).
[3] M. B. James *et al.*, IEEE Trans. Nucl. Sci. **30**, 2992 (1983).
[4] L. Serafini and M. Ferrario, in *Physics of, and Science with, the X-Ray Free-Electron Laser*, edited by S. C. M. C. I. Lindau and C. Pellegrini, AIP Conf. Proc. No. 581 (AIP, New York, 2001), p. 581.
[5] X. J. Wang *et al.*, Phys. Rev. E **54**, R3121 (1996).
[6] K. J. Gaffney and H. N. Chapman , Science **316**, 1444 (2007).
[7] J. T. Seeman, IEEE Trans. Nucl. Sci. **30**, 3180 (1983).
[8] K. L. F. Bane, P. Chen, and P. B. Wilson, IEEE Trans. Nucl. Sci. **32**, 3524 (1985).
[9] A. G. Ruggiero *et al.*, in *Advanced Accelerator Concepts: 3rd Workshop*, edited by F. E. Mills, AIP Conf. Proc. No. 156 (AIP, New York, 1986), p. 247.
[10] P. Schutt, T. Weiland, and V. M. Tsakanov, in *Proceedings of the Second All-Union Conference on New Methods of Charged Particle Acceleration* (Springer, New York, 1989).
[11] C. Jing *et al.*, Phys. Rev. Lett. **98**, 144801 (2007).
[12] J. B. Rosenzweig *et al.*, Phys. Scr. **T30**, 110 (1990).
[13] R. Maeda, Phys. Rev. ST Accel. Beams **7**, 111301 (2004).
[14] D. H. Dowell *et al.*, Appl. Phys. Lett. **63**, 2035 (1993).
[15] M. E. Conde *et al.*, Phys. Rev. ST Accel. Beams **1**, 041302 (1998).
[16] D. C. Nguyen and B. E. Carlsten, Nucl. Instrum. Methods Phys. Res., Sect. A **375**, 597 (1996).
[17] L. Serafini, IEEE Trans. Plasma Sci. **24**, 421 (1996).
[18] M. Boscolo *et al.*, Nucl. Instrum. Methods Phys. Res., Sect. A **577**, 409 (2007).
[19] D. Palmer, in *Advanced Accelerator Concepts: Seventh Workshop*, edited by S. Chattopadhyay, AIP Conf. Proc. No. 398 (AIP, New York, 1997), p. 695.
[20] Here we use the first-order expression $R_{56} = \int \frac{\eta(s')}{\rho(s')} ds'$, where ρ is the local radius of curvature of the beam trajectory. With this definition, the dogleg has $R_{56} < 0$ and bunches with the front at low energy and the back at high energy are compressed and vice versa.
[21] http://mad.web.cern.ch/mad/.
[22] M. Ter-Mikaelian, *High-Energy Electromagnetic Processes in Condensed Media* (Willey-Interscience, New York, 1972).
[23] E. Kallos *et al.*, in *Proceedings of the Particle Accelerator Conference 07*, http://accelconf.web.cern.ch/AccelConf/p07/PAPERS/THPMS031.PDF.